arXiv:1409.3962v1 [cond-mat.soft] 13 Sep 2014

# A Study of Snake-like Locomotion Through the Analysis of a Flexible Robot Model

Giancarlo Cicconofri and Antonio DeSimone
SISSA, International School of Advanced Studies
Via Bonomea 265, 34136 Trieste - Italy
giancarlo.cicconofri@sissa.it , desimone@sissa.it

**Abstract**

We examine the problem of snake-like locomotion by studying a system consisting of a planar inextensible elastic rod that is able to control its spontaneous curvature. Using a Cosserat model we derive, through variational principles, the equations of motion for two special cases: one in which the system is confined inside a frictionless channel, and one in which it is placed in an anisotropic frictional environment, modeling the dynamical setting of the slithering of snakes on flat surfaces. The presence of constraints in both cases leads to non-standard boundary conditions, that allow us to close the equations of motion reducing them to a differential and an integro-differential equation, respectively, for one end point (the tail) of the active rod. For the snake-like case we also provide analytic solutions for a special class of motions. We highlight the role of the spontaneous curvature in the pushing (and the steering, in the snake-like setting) needed to power locomotion. Comparisons with available experiments confirm that the model is able to capture many of the essential findings in the zoological literature. The complete solvability and the existence of analytic solutions offers a tool that may prove valuable for the design of bio-inspired soft robots.

**Keywords** Snake Locomotion, Undulatory Locomotion, Soft Robotics, Cosserat Rod Models, Bio-inspired Robots

# Contents

**1 Introduction** **3**

**2 The Flexible Robot Model** **4**

**3 Sliding Inside a Channel** **6**
3.1 Derivation of the Equations of Motion . . . . . 6
3.2 Discussion of the results . . . . . 8

**4 Snake-like Locomotion** **10**
4.1 Derivation of the Equations of Motion . . . . . 10
4.2 A Class of Serpentine Solutions . . . . . 13

**5 Discussion** **18**

# 1 Introduction

Snake locomotion has fascinated natural scientists for a long time. More recently, it has become a topic of great interest as one of the key examples of soft bio-inspired robotics. This is a new and recent paradigm in robotic science [1, 2], whereby inspiration is sought from nature to endow robots with new capabilities in terms of dexterity (think, for example, of the manipulation abilities of an elephant trunk or of an octopus arm) and adaptability (think, for example, of the ability of snakes to handle unexpected interactions with unstructured environments and move successfully on uneven terrains by adapting their gait to ground properties that change from place to place in an unpredictable way).

The way snakes move has been the subject of seminal works by Gray [3, 4], see also [5, 6]. In these early studies Gray described the mechanics underlying snake locomotion inside closely fitting channels and, more broadly, snake propulsion on a surface in the presence of external push-points. Since then more refined measurements have been reported in the zoological literature focusing on the same kind of experiments. Work of interest for us includes [7], containing a coupled analysis of muscular activity and forces transmitted by snakes to arrays of pegs among which they move. Just recently, the focus has turned to the importance of frictional anisotropy of snake ventral skin on surfaces as a mean of self-propulsion, stimulating both experimental [8, 9, 10, 11] and theoretical research [10, 11, 12].

The idea that frictional anisotropy plays a role in snake locomotion was put forward long ago in the engineering literature [5] (theory) and, most notably, by Hirose in his seminal work on robotic snake-like locomotion [13]. Hirose was among the first to call attention on the potential of biological inspiration in designing robots by studying snake-like locomotors and manipulators [13]. Technological advances in this field have led to the development of detailed models for snake robots crafted with more and more jointed active parts, eventually leading to the use of continuum theories [14]. In some more recent contributions on the subject [15, 16, 17, 18] Cosserat models are used for the mechanics of slender flexible robots, described as deformable rods.

In this paper, we study a model system consisting of a planar inextensible elastic rod that is able to control its spontaneous curvature. We use a Cosserat model, and derive the equations of motion for two special cases: one in which the system is confined inside a frictionless sleeve, and one in which the system is placed on an anisotropic frictional environment with an infinite contrast between longitudinal and transversal friction, so that the rod can slide longitudinally along its axis, but cannot slip laterally (i.e., in the transversal direction).

Our model is related to the ones studied in [10, 11, 12], with some simplifying assumptions. We neglect the possibility of lateral slipping and we do not consider lifting of portions of the body (and the corresponding modulation of frictional forces) as in [10] where, however, the resulting curvature is assumed controllable while in our model only the spontaneous curvature is prescribed (and the observed curvature emerges from the elastic balance with bending stiffness and forces transmitted by the ground surface). We also do not consider internal viscous dissipations and nonlinearities of the longitudinal frictional force, as done in [12] where, however, only periodic solutions are studied and the equations are closed by imposing an ansatz on some dynamical quantities. This allows us to obtain explicit analytic solutions in the case of snakes/rods

of finite size (thus, we are not restricted to numerical simulations or to periodic solutions), and also to prove existence and uniqueness of solutions of the equation of motions we derive. For studies of undulatory swimming locomotion conducted in a similar spirit, see [19, 20, 21].

Our main results are the following. In the case of the robot placed inside a channel we are able to reduce the system of equations to a simple ordinary differential equation for the end point coordinate only (the only degree of freedom that an inextensible rod has when forced to slide inside a predetermined path). Such an equation enables us to demonstrate how a flexible robot can actively propel itself inside a channel provided that such a channel exhibits a variation of curvature along its track, putting in a quantitative framework the experimental and theoretical findings in snake motility by Gray in [3]. In the case of the robot placed on an anisotropic frictional environment we can provide a wide class of explicit "serpentine" solutions (with constant longitudinal velocity, sinusoidal observed curvature and a straight axis of locomotion). Within this class we can show how different spontaneous curvature histories can produce the very same motion and show how some of them qualitatively reflect the experimental measurements performed on real snakes in [7].

Another particularly interesting outcome of our analysis in this case is the emergence of an asymmetry in the mechanical boundary conditions at the (leading) head and the (trailing) tail. This is not only a mathematical subtlety, but it is also deeply grounded in the physics of the problem. While the tail follows a path predetermined by the preceding interior points, the head is free to veer laterally. This is reflected in the action of the spontaneous curvature which can in turn be regarded as a sum of two components: one that provides the pushing action and another one, concentrated near the head, that is responsible for the steering.

The paper is organized as follows. In Section 2 we formulate our mathematical model of flexible robot. In Section 3 we derive the governing equations and the appropriate boundary conditions for motion inside a frictionless tube or channel, solve them in some simple geometries, and discuss their physical implications. In Section 4 we derive the governing equation and corresponding boundary conditions for the planar motion of our on an anisotropic frictional environment, and propose a class of analytical serpentine solutions. A discussion of the relevance of our results in the context of biological snake locomotion or in the context of bio-inspired snake-like robotic locomotion is contained in the Discussion section, while the existence and uniqueness of the solution of the equation of motion is proved in the Appendix.

# 2 The Flexible Robot Model

We consider a model consisting of a (long) chain of cross shaped elements (Fig. 1.B) linked together by ideal joints connected by deformable springs. We assume that each spring is able to actively change its equilibrium length. Following [16, 15, 17, 18] we model this system through a continuous description based on the planar Cosserat rod theory.

A configuration of a Cosserat rod of reference length $L$ on the plane is defined by a pair of vector-valued functions

$$[0, L] \times [0, \infty) \ni (s, t) \mapsto \mathbf{r}(s, t)\,,\ \mathbf{b}(s, t) \tag{1}$$

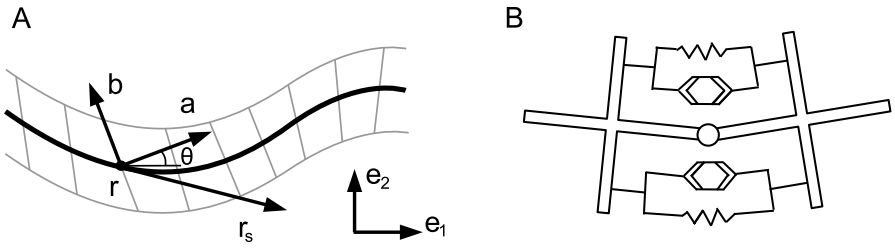


Figure 1: A) Variables describing a Cosserat rod configuration. B) Schematic model for the constitutive elements of the robot's structure.

where $\mathbf{b}$ is a unit vector (Fig. 1.A). As in [22] we introduce also the unit vector $\mathbf{a} := -\mathbf{e}_3 \times \mathbf{b}$, where $\mathbf{e}_3$ is the unit vector normal to the plane. We then define the *strain* variables $\nu$ and $\eta$ through the following decomposition along the moving orthonormal frame $\{\mathbf{a}, \mathbf{b}\}$

$$\mathbf{r}_s = \nu\mathbf{a} + \eta\mathbf{b}$$

where the subscript $s$ is used to denote the partial derivative with respect to the space variable. The function $\nu = \nu(s,t)$ describes the *stretch*, while $\eta = \eta(s,t)$ defines the *shear* strain. Finally the *bending* strain $\mu := \theta_s$ is obtained through the scalar valued function $\theta(s,t)$ defined by

$$\mathbf{a}(s,t) = \cos\theta(s,t)\mathbf{e}_1 + \sin\theta(s,t)\mathbf{e}_2$$

where $\{\mathbf{e}_1, \mathbf{e}_2\}$ is a fixed basis in the plane containing the rod. We consider our system as being made of an infinite number of elements like the ones in Fig 1.B, each of them being of infinitesimal length, and assembled along the central curve $\mathbf{r}$ of the rod. Since we assume them to be rigid, we impose the constraints that the rod is inextensible and unshearable:

$$\nu(s,t) = 1 \quad \text{and} \quad \eta(s,t) = 0\,. \tag{2}$$

The ability of the robot to modify the equilibrium length of each of the connecting springs can be naturally modeled macroscopically by considering an elastic medium which can actively vary its spontaneous curvature. We model this by introducing the elastic potential density

$$\mathcal{U}(\mu, s, t) = \frac{EJ}{2}\big(\mu - \alpha(s,t)\big)^2 \tag{3}$$

where $EJ$ is the bending stiffness of the robot. Notice that if (2) hold, then $\mathbf{r}_s$ always coincides with the unit vector $\mathbf{a}$, and the bending strain $\mu(s,t)$ is equal to the curvature of the rod at the point $\mathbf{r}(s,t)$. The function $\alpha$ in (3) therefore can be viewed as the varying spontaneous curvature, which we assume to be freely controllable in order to set the robot in motion. Along with the elastic potential we define also the kinetic energy density

$$\mathcal{T}(\mathbf{r}_t, \theta_t) = \frac{\rho A}{2}\,\mathbf{r}_t \cdot \mathbf{r}_t + \frac{\rho J}{2}\,\theta_t^2$$

where the subscript $t$ denotes the partial derivative with respect to time, $\rho A$ is the linear mass density and $\rho J$ the linear moment of inertia. Finally, the

Lagrangian density $\mathcal{L}$ of the system reads

$$\mathcal{L} = \mathcal{T} - \mathcal{U} - \widetilde{N}(\nu - 1) - \widetilde{H}\eta \tag{4}$$

where $\widetilde{N} = \widetilde{N}(s,t)$ and $\widetilde{H} = \widetilde{H}(s,t)$ are the reactive internal tractions (axial tension and shear force, respectively) enforcing constraints (2).

# 3 Sliding Inside a Channel

The first problem we formulate in the context of our model is motion inside a frictionless pipe or channel. We place our robot inside a curved channel fitting exactly its body, assuming there is no contact friction between the walls of the channel and the robot itself. We model such a setting by imposing the external constraint

$$\mathbf{r} \in \text{Graph}\,\{\mathbf{\Gamma}\} \quad \text{or} \quad \phi^{\Gamma}(\mathbf{r}) = 0 \tag{5}$$

where the equation $\phi^{\Gamma} = 0$ defines (we assume, globally) the curve $\mathbf{\Gamma}$ which we interpret as the central line of the channel. There is no loss of generality in assuming $|\nabla\phi^{\Gamma}| = 1$.

## 3.1 Derivation of the Equations of Motion

We derive the equations of motion through Hamilton's Principle, adding to (4) an external reactive potential $-\tilde{f}\phi^{\Gamma}(\mathbf{r})$, where $\tilde{f} = \tilde{f}(s,t)$ is the Lagrange multiplier enforcing (5). A solution $(\mathbf{r}, \theta)$ must satisfy

$$\delta \int_{t_1}^{t_2}\int_{0}^{L} \mathcal{L} - \tilde{f}\phi^{\Gamma}(\mathbf{r})\; ds dt = 0 \tag{6}$$

for every variations $\delta\mathbf{r}$ and $\delta\theta$ defined on $[0, L] \times [t_1, t_2]$ and vanishing at its boundary. If we define the active moment $M^{\alpha} = EJ(\theta_s - \alpha)$ and $\widetilde{\mathbf{n}} = \widetilde{N}\mathbf{a} + \widetilde{H}\mathbf{b}$, the Euler-Lagrange equations we obtain from (6) are

$$\begin{aligned} \widetilde{\mathbf{n}}_s - \tilde{f}\nabla\phi^{\Gamma}(\mathbf{r}) &= \rho A\, \mathbf{r}_{tt} \\ M^{\alpha}_s \mathbf{e}_3 + \mathbf{r}_s \times \widetilde{\mathbf{n}} &= \rho J \theta_{tt} \mathbf{e}_3 \end{aligned}$$

To close the equations of motion we rely on the so called Principle of Mechanical Boundary Conditions (from now on: PoMBC) [23]. This principle is used to deal with systems subjected to kinematical constraints at the edges. It furnishes a method to define *generalized* edge loads acting on the system by considering the rate at which work is expended in virtual motions compatible with the constraints, and it states that all *generalized* edge loads acting on the system must be explicitly prescribed.

Compatibly with the global requirement (5), we suppose that the configuration $(\mathbf{r}, \theta)$ satisfies the following relations at the edges

$$\mathbf{r}(0,t) = \mathbf{\Gamma}(s_0(t)), \mathbf{r}(L,t) = \mathbf{\Gamma}(s_L(t)), \theta(0,t) = \Theta(s_0(t)), \theta(L,t) = \Theta(s_L(t)) \tag{7}$$

where $s_0$ and $s_L$ are the curvilinear coordinates relative to $\mathbf{\Gamma}$ of the two ends of the rod, which we call *generalized edge coordinates*, and $\Theta$ is the angle between the tangent vector to $\mathbf{\Gamma}$ and $\mathbf{e}_1$, so that

$$\mathbf{\Gamma}(s) = \mathbf{\Gamma}(\xi_0) + \int_{\xi_0}^{s} \cos\Theta(\lambda)\mathbf{e}_1 + \sin\Theta(\lambda)\mathbf{e}_2\; d\lambda\,. \tag{8}$$

Now, following the PoMBC, we write the work rate $P_{\text{edge}}$ of the edge loads as

$$P_{\text{edge}} = \widetilde{\mathbf{n}}(s,t)\cdot\mathbf{r}_t(s,t)\Big|_{s=0}^{s=L} + M^{\alpha}(s,t)\theta_t(s,t)\Big|_{s=0}^{s=L}. \tag{9}$$

Using (7) to derive the expressions for $\mathbf{r}_t$ and $\theta_t$ at $s=0,L$ we obtain

$$\begin{aligned} P_{\text{edge}} \;=\; & \dot{s}_L(t)\Big(\widetilde{\mathbf{n}}(L,t)\cdot\boldsymbol{\Gamma}_s(s_L(t)) + M^{\alpha}(L,t)k^{\Gamma}(s_L(t))\Big) \\ & -\dot{s}_0(t)\Big(\widetilde{\mathbf{n}}(0,t)\cdot\boldsymbol{\Gamma}_s(s_0(t)) + M^{\alpha}(0,t)k^{\Gamma}(s_0(t))\Big) \end{aligned}$$

where we used a "dot" to denote the time derivative of the generalized coordinates, and $k^{\Gamma}$ is the curvature of $\boldsymbol{\Gamma}$. The coefficients multiplying the *generalized velocities* $\dot{s}_0(t)$ and $\dot{s}_L(t)$ are the *generalized edge loads* which, by the PoMBC, have to be prescribed. Since we suppose that no external edge forces are doing work on the system, we enforce the condition $P_{\text{edge}}=0$ by setting such loads equal to zero.

Finally, conditions (2) and (5) must be added to the equations of the system.

Now, since we assume our robot to be inextensible and unshearable, and since the backbone curve $\mathbf{r}$ of the robot is forced inside the graph of $\boldsymbol{\Gamma}$, we see that the constrained system can be described with only one degree of freedom, namely the curvilinear coordinate relative to $\boldsymbol{\Gamma}$ of the first end of the robot. Thus,

$$\mathbf{r}(s,t) = \boldsymbol{\Gamma}(s_0(t)+s) \quad \text{and} \quad \theta(s,t) = \Theta(s_0(t)+s)\,.$$

Substituting these expressions in the equations of motion we obtain

$$\begin{aligned} & \widetilde{N}_s - k^{\Gamma}\widetilde{H} = \rho A\,\ddot{s}_0(t) \\ & k^{\Gamma}\widetilde{N} + \widetilde{H}_s - \tilde{f} = \rho A\,k^{\Gamma}\dot{s}_0(t)^2 \\ & EJ(k^{\Gamma}_s - \alpha_s) + \widetilde{H} = \rho J(k^{\Gamma}\ddot{s}_0(t) + k^{\Gamma}_s\dot{s}_0(t)^2) \end{aligned} \tag{10}$$

where $k^{\Gamma} = k^{\Gamma}(s_0(t)+s)$. As for the boundary conditions they now read

$$\begin{aligned} & \widetilde{N}(0,t) + EJ\big(k^{\Gamma}(s_0(t)) - \alpha(0,t)\big)k^{\Gamma}(s_0(t)) = 0 \\ & \widetilde{N}(L,t) + EJ\big(k^{\Gamma}(s_0(t)+L) - \alpha(L,t)\big)k^{\Gamma}(s_0(t)+L) = 0 \end{aligned} \tag{11}$$

We show now that the system we found is equivalent to an ODE for $s_0(t)$. If we substitute the expression of $\widetilde{H}$ given by third equation in the first one in (10) then, integrating on the space variable, we have

$$\begin{aligned} m\ddot{s}_0 &= \widetilde{N}\Big|_0^L + EJ\int_0^L (k^{\Gamma}_s - \alpha_s)k^{\Gamma}\,ds - \rho J\,R^{\Gamma}(\dot{s}_0(t), s_0(t)) - \rho J\,Q^{\Gamma}(s_0(t))\ddot{s}_0(t) \\ &= \widetilde{N}\Big|_0^L + EJ(k^{\Gamma}-\alpha)k^{\Gamma}\Big|_0^L - EJ\int_0^L (k^{\Gamma}-\alpha)k^{\Gamma}_s\,ds - \rho J\,R^{\Gamma} - \rho J\,Q^{\Gamma}\ddot{s}_0(t) \end{aligned}$$

where $m = \int_0^L \rho A ds$ is the total mass of the robot, and

$$\begin{aligned} R^{\Gamma}(\dot{s}_0(t), s_0(t)) &= \frac{\dot{s}_0(t)^2}{2}\left(k^{\Gamma}(s_0(t)+L)^2 - k^{\Gamma}(s_0(t))^2\right) \\ Q^{\Gamma}(s_0(t)) &= \int_0^L k^{\Gamma}(s_0(t)+s)^2 ds\,. \end{aligned}$$

If we now apply (11) we obtain the equation

$$\begin{aligned}\big(m+\rho J\,Q^{\Gamma}(s_0(t))\big)\,\ddot{s}_0(t) &= \frac{EJ}{2}\left(k^{\Gamma}(s_0(t))^2-k^{\Gamma}(s_0(t)+L)^2\right)\\ &\quad -\rho J\,R^{\Gamma}(\dot{s}_0(t),s_0(t))+EJ\int_0^L\alpha(s,t)\,k^{\Gamma}_s(s_0(t)+s)\,ds \quad (12)\end{aligned}$$

which, complemented with initial position and velocity, defines $s_0$ uniquely. After that also the shear force $\widetilde{H}$ is uniquely defined by the third equation in (10), while

$$\begin{aligned}\widetilde{N}(s,t) &= \int_0^s\Big\{\rho A\,\ddot{s}_0(t)+k^{\Gamma}(s_0(t)+\lambda)\widetilde{H}(\lambda,t)\Big\}\,d\lambda\\ &\quad -EJ\big(k^{\Gamma}(s_0(t))-\alpha(0,t)\big)k^{\Gamma}(s_0(t))\,.\end{aligned}$$

Using all the above expressions we can recover $\tilde{f}$ from the second equation in (10).

## 3.2 Discussion of the results

Let us suppose that our robot is stiff and slender enough, such that $EJ, \rho A \gg \rho J$. With these assumptions it is reasonable to neglect the terms containing $\rho J$ in (12), obtaining the simplified equation

$$m\ddot{s}_0(t)=\frac{EJ}{2}\left(k^{\Gamma}(s_0(t))^2-k^{\Gamma}(s_0(t)+L)^2\right)+EJ\int_0^L\alpha(s,t)\,k^{\Gamma}_s(s_0(t)+s)\,ds \quad (13)$$

Here the continuum system is reduced to an equivalent equation of a point particle of mass $m$ subjected to a force given by the sum of the two terms on the right hand side of (13). The first term is a "potential" force depending exclusively on the geometry of $\mathbf{\Gamma}$, while the second one is an "active" force which depends also on the spontaneous curvature $\alpha$.

Let us consider only the first one by setting $\alpha = 0$. The system described in this case is a passive elastic rod with straight rest configuration placed inside a curved channel. We see that the force the rod is subjected to depends only on the curvature of the channel at the two ends of the body. This can be interpreted as a consequence of inextensibility. Moreover we can see that the sign of the force is such that the rod is always pushed towards the region of smaller curvature. Consider as an example what happens in the case in which the channel is shaped like a spiral segment (see Fig.2). If we take $k^{\Gamma}(s) = 1/s$ then (13) with $\alpha = 0$ reads

$$m\ddot{s}_0(t)=-U'(s_0(t)) \quad \text{where} \quad U(s_0)=\frac{EJL}{2(s_0+L)s_0}\,.$$

In order to thread the rod inside the spiral by varying the coordinate of the end point from $\xi_2$ to $\xi_1$ we need to perform a positive work

$$W=U(\xi_1)-U(\xi_2)=\frac{EJ}{2}\left(\frac{L}{(\xi_1+L)\xi_1}-\frac{L}{(\xi_2+L)\xi_2}\right)>0 \qquad (14)$$

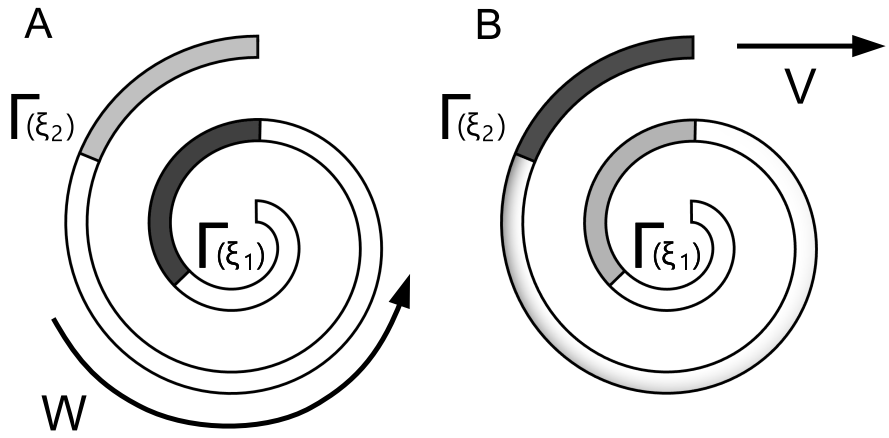


Figure 2: A) Two configurations of the elastic rod inside a spiral channel: initial (light grey) and final (dark grey). A positive work $W$ is necessary to vary the coordinate of the end point from $\mathbf{\Gamma}(\xi_2)$ to $\mathbf{\Gamma}(\xi_1)$ and force the rod inside the channel. B) Upon release, the first end point slides back from $\mathbf{\Gamma}(\xi_1)$ to $\mathbf{\Gamma}(\xi_2)$ and the rod exits the channel with velocity $V$.

since we have to increase the curvature at every point of the body. If we then release the rod it will accelerate towards the exit and return back to $\xi_2$ with a positive velocity

$$V = \sqrt{\frac{EJ}{m}\left(\frac{L}{(\xi_1+L)\xi_1} - \frac{L}{(\xi_2+L)\xi_2}\right)} > 0\,. \tag{15}$$

In other words, the system moves towards a "straighter" configuration, decreasing its elastic energy and therefore increasing its kinetic energy. Similar problems of passive elastic rods sliding inside frictionless sleeves have been studied, both analytically and experimentally, in [24].

Let us suppose now that $\alpha \neq 0$. In the case of a spiral channel the active force term in (13) can assume any value if we suppose that we have no restrictions in the choice of $\alpha$. This means, in particular, that an active elastic robot can slide *inside* the spiral without need of external pushing. More generally, our robot can achieve motion in a predetermined direction when placed inside any channel which does not present circular or straight sections of length greater than $L$.

This last result, in particular, is reminiscent of the theoretical and experimental findings of J. Gray in [3]. He describes the muscular and vertebral structure of a typical snake with a discrete model that is closely related to ours. Using an energy balance argument, he concludes that it is possible for a snake to slide inside a channel only provided such a channel exhibits a variation of curvature along its track. To test his theoretical predictions he confines a specimen of *Tropidonotus natrix* inside closely fitting rigid tubes with different shapes. While the animal is able to slide inside a sinusoidal one, it changes completely its locomotion strategy when placed in a straight tube, provided that the tube is sufficiently wide. In this case the snake adopts a so called "concertina" move-

ment, propelling itself thanks to contact friction with the surrounding walls. Such concertina movement, however, becomes impossible in a straight tube exactly matching the body width of the snake.

# 4 Snake-like Locomotion

We use now our model to discuss the locomotion of snakes and biomimetic snake-like devices moving on a plane while subjected to an anisotropic frictional environment. As in [12], we suppose that no slip occurs in the transversal direction, that is

$$\mathbf{r}_s^{\perp} \cdot \mathbf{r}_t = 0 \tag{16}$$

where $\mathbf{r}_s^{\perp} = \mathbf{e}_3 \times \mathbf{r}_s$. We denote by $-\tilde{f}\mathbf{r}_s^{\perp}$ the transversal reactive force per unit length (exerted by the ground on the snake) enforcing the no-slip condition, where $\tilde{f}$ is the Lagrange multiplier associated with constraint (16). At the same time, we suppose that a frictional force $\mathbf{F}^{//}$ acts in the longitudinal direction

$$\mathbf{F}^{//} = -\gamma^{//} \frac{\mathbf{r}_s}{|\,\mathbf{r}_s\,|} \mathrm{Sgn}(\mathbf{r}_t \cdot \mathbf{r}_s)\,.$$

Real snakes [8, 9, 10], as well as real snake-like robots [13], cannot rely on transversal frictional reactions of arbitrary magnitude to avoid lateral slipping. The theory we present here, therefore, must be complemented with suitable selection of its results. Solutions reasonably describing realistic systems can be considered those for which the reactive force imposing the constraint (16) does not exceed a maximum value, which can be determined experimentally.

## 4.1 Derivation of the Equations of Motion

We deduce the equations of motion through the Lagrange-d'Alembert principle, which has been recently applied to describe elastic systems in perfect friction contact [25] and elastic systems rolling without sliding on a substrate [26]. The principle states that a solution $(\mathbf{r}, \theta)$ subjected to the dissipative force $\mathbf{F}^{//}$ and that satisfies the constraint (16) must solve

$$\delta \int_{t_1}^{t_2}\int_0^L \mathcal{L}\, ds dt + \int_{t_1}^{t_2}\int_0^L \mathbf{F}^{//} \cdot \delta\mathbf{r}(s,t)\, ds dt = 0 \tag{17}$$

for every variations $\delta\mathbf{r}$ and $\delta\theta$ that vanish at the boundary of $[0, L] \times [t_1, t_2]$, while $\delta\mathbf{r}$ also satisfy

$$\mathbf{r}_s^{\perp} \cdot \delta\mathbf{r} = 0\,. \tag{18}$$

Calculating the variation on the left hand side of (17), after integration by parts and reordering, we have

$$\begin{aligned}
&\delta \int_{t_1}^{t_2}\int_0^L \mathcal{L}\, ds dt + \int_{t_1}^{t_2}\int_0^L \mathbf{F}^{//} \cdot \delta\mathbf{r}(s,t)\, ds dt = \\
&\int_{t_1}^{t_2}\int_0^L \left\{ -\rho A\, \mathbf{r}_{tt} + (\widetilde{N}\mathbf{a})_s + (\widetilde{H}\mathbf{b})_s + \mathbf{F}^{//} \right\} \cdot \delta\mathbf{r}\, ds dt \\
+ &\int_{t_1}^{t_2}\int_0^L \left\{ -\rho J \theta_{tt} + EJ(\theta_{ss} - \alpha_s) + (\nu\widetilde{H} - \eta\widetilde{N}) \right\} \delta\theta\, ds dt
\end{aligned}$$

Since (17) holds for all the variations satisfying (18), it forces the coefficient multiplying $\delta\theta$ to vanish, while the coefficient relative to $\delta\mathbf{r}$ must take the form $\tilde{f}\mathbf{r}_s^{\perp}$, where $\tilde{f} = \tilde{f}(s,t)$ is the unknown Lagrange multiplier enforcing the constraint (16). The equations of motion then read

$$\begin{aligned} \widetilde{\mathbf{n}}_s + \mathbf{F}^{//} - \tilde{f}\mathbf{r}_s^{\perp} &= \rho A\, \mathbf{r}_{tt} \\ M_s^{\alpha}\mathbf{e}_3 + \mathbf{r}_s \times \widetilde{\mathbf{n}} &= \rho J \theta_{tt}\mathbf{e}_3 \end{aligned}$$

We complement these equations with boundary conditions by relying again on the PoMBC. In contrast with what we did in the previous section, instead of introducing generalized edge coordinates first, we give directly the expressions for $\mathbf{r}_t$ and $\theta_t$ at the two ends in terms of generalized edge velocities. We do that through the following heuristic argument.

Let us consider a typical configuration of the robot in motion while subjected to the external constraint (16). We suppose that such a movement is directed head-first, where we denote the head as $\mathbf{r}(L,t)$ and the tail as $\mathbf{r}(0,t)$. What happens to the configuration of the edges between two successive instants is then illustrated in Fig.3. An asymmetry between head and tail emerges. Because of (16), the tail position and director can change only by assuming the values previously taken by an adjacent internal point. We can therefore impose on $s = 0$ the same conditions we had in the channel case, namely,

$$\mathbf{r}_t(0,t) = v_0(t)\,\mathbf{r}_s(0,t) \quad \text{and} \quad \theta_t(0,t) = v_0(t)k(0,t)$$

where $v_0$ is the (only) generalized velocity at $s = 0$ and $k(0,t)$ is the curvature of $\mathbf{r}$ evaluated in $s = 0$ at time $t$. As for the head configuration we see that, since the path is no longer predetermined, we have an extra degree of freedom. We must assume $\mathbf{r}_t$ to be collinear to $\mathbf{r}_s$, therefore this extra degree of freedom must come from the rotation of the director. We then impose

$$\mathbf{r}_t(L,t) = v_L(t)\,\mathbf{r}_s(L,t) \quad \text{and} \quad \theta_t(L,t) = \omega_L(t)$$

where $v_L$ and $\omega_L$ are the generalized velocities for the system at $s = L$. The work rate of the external edge forces is

$$\begin{aligned} P_{\text{edge}} &= \widetilde{\mathbf{n}}(L,t)\cdot\mathbf{r}_s(L,t)v_L(t) + M^{\alpha}(L,t)\omega_L(t) \\ &\quad -\Big(\widetilde{\mathbf{n}}(0,t)\cdot\mathbf{r}_s(L,t) + M^{\alpha}(0,t)k(0,t)\Big)\,v_0(t)\,. \end{aligned}$$

Thus, we see that there are two generalized edge loads at $s = L$, namely, the axial tension $\widetilde{\mathbf{n}}\cdot\mathbf{r}_s$ and the active moment $M^{\alpha}$, and one at $s = 0$, with the same expression it had in the channel case. We prescribe them to vanish because, just like in previous section, we suppose that no external edge force is doing work on the system.

Alongside with the boundary conditions coming from the vanishing of the generalized edge loads, the system must be complemented with equations (2) and (16).

The nonholonomic condition (16) compels the robot to move within a curve in the plane, much like it was for the channel case in the previous section. This time, however, the path is not a-priori determined but is created during the motion, and it is an unknown of the problem. In fact, the constraints (2) and

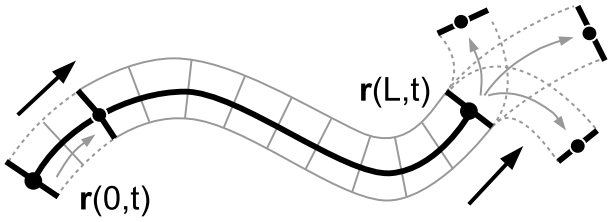


Figure 3: Typical configuration of the robot moving while subjected to the nonholonomic constraint (16). Arrows indicate the direction of motion. Tail position and director change by assuming the values taken previously at an internal point. The head configuration has an extra degree of freedom, since it is allowed to turn freely.

(16) lead to the existence of some function $s_0$ and *some* curve $\mathbf{\Gamma}$, which have *both* to be determined, such that

$$\mathbf{r}(s,t) = \mathbf{\Gamma}(s_0(t)+s) \quad \text{and} \quad \theta(s,t) = \Theta(s_0(t)+s)\,,$$

where $\Theta$ is defined by (8). Since the boundary conditions we derived hold only for head-first motions, we only consider solutions satisfying

$$\dot{s}_0(t) > 0\,. \tag{19}$$

The equations of motion written in components then read

$$\begin{aligned} \widetilde{N}_s - k\widetilde{H} - \gamma'' &= \rho A\, \ddot{s}_0(t) \\ k\widetilde{N} + \widetilde{H}_s - \tilde{f} &= \rho A\, k\, \dot{s}_0(t)^2 \\ EJ(k_s - \alpha_s) + \widetilde{H} &= \rho J(k\, \ddot{s}_0(t) + k_s\, \dot{s}_0(t)^2) \end{aligned} \tag{20}$$

where $k = k(s_0(t)+s)$ is the curvature of $\mathbf{\Gamma}$ at the point $s_0(t)+s$.

We close the equations through the boundary conditions obtained by setting the generalized edge loads to zero

$$\begin{aligned} &\widetilde{N}(0,t) + EJ(k(s_0(t)) - \alpha(0,t))k(s_0(t)) = 0 \\ &\widetilde{N}(L,t) = 0\,,\ k(s_0(t)+L) = \alpha(L,t) \end{aligned} \tag{21}$$

and by prescribing initial values for $s_0$ and $\dot{s}_0$ at $t = t_0$, together with the initial curvature $k(s_0(t_0)+s) = K(s)$ with $s \in [0, L]$. Such values must satisfy the compatibility relations

$$\dot{s}_0(t_0) > 0 \quad , \quad K(L) = \alpha(L, t_0) \quad \text{and} \quad K'(L)\dot{s}_0(t_0) = \dot{\alpha}(L, t_0)\,. \tag{22}$$

Under these conditions we can prove existence of a unique solution of (20), which lead to solution for $\mathbf{r}$ and $\theta$ once the initial point $\mathbf{r}(0,t_0)$ and the initial orientation $\theta(0,t_0)$ of the first end are prescribed. The detailed proof is provided in the Appendix. We only stress here the fact that the problem can be reduced to an integro-differential equation for the variable $s_0$ alone, while all the other unknowns can be deduced consequentially. In particular, the curvature $k$ can

be deduced from $s_0$ through the third boundary condition in (21), which comes from the vanishing of the active moment $M^\alpha$ at the leading edge. This latter condition, namely,

$$k(s_0(t) + L) = \alpha(L, t) \tag{23}$$

assigns a crucial role to the active curvature in the determination of the geometry of the path followed by the robot. Thus, the value of $\alpha$ at $s = L$ operates as a "steering wheel" while the internal values of the spontaneous curvature supply the active force for propulsion, as it was for the channel case. The following section provides an illustrative example of these two key mechanisms.

## 4.2 A Class of Serpentine Solutions

We discuss now some explicit solutions to the snake-like locomotion equations. In order to construct them, we use an "inverse kinematics" approach, namely, we prescribe the motion (trajectory and speed, through the assignment of $k(s, t)$ and $\dot{s}_0(t)$) of the snake, and we look for a history of spontaneous curvatures that produces it, i.e., a function $\alpha(s, t)$ that solves equations (20) with boundary conditions (21) together with the prescribed $k(s, t)$ and $\dot{s}_0(t)$. It is easy to see that the solution to our "inverse kinematics" problem is not unique. In fact, we will exhibit two such spontaneous curvature histories producing the same motion (accompanied by different transversal forces).

We consider solutions corresponding to a constant longitudinal velocity

$$V = \dot{s}_0(t)$$

together with the following serpentine $L$-periodic curvature history

$$k(s, t) = \zeta \sin\Big(\frac{s}{\lambda} + Vt\Big) \quad \text{where } \lambda = \frac{L}{2\pi n}\,. \tag{24}$$

The geometry of the curve $\Gamma$ that our robot is following is then uniquely determined up to a rotation and a translation on the plane, leading to a "serpentine" path like the one depicted in Fig.4. In particular, the solution $\mathbf{r}(s, t)$ associated with (24) with $\mathbf{r}(0, 0) = \mathbf{0}$ and oscillating around an axis parallel to $\mathbf{e}_1$ is given by

$$\mathbf{r}(s, t) = \int_0^{s+\lambda V t} \cos\Theta(\xi)\mathbf{e}_1 + \sin\Theta(\xi)\mathbf{e}_2\, d\xi \quad \text{where} \quad \Theta(\xi) = -\zeta\lambda\cos\left(\frac{\xi}{\lambda}\right).$$

The velocity $V$, the number of turns of the body $n$ and the coefficient $\zeta$ are free parameters. We remark that for small values of the geometric parameter $\zeta$, the path followed by the snake becomes close to a straight line, while as $\zeta$ grows, the paths become wavier and wavier. We suppose that $\zeta$ is small enough in order to avoid self-intersections.

A possible solution for $\alpha$ is given by

$$\alpha(s, t) = \sigma\Big(\cos\Big(\frac{s}{\lambda} + Vt\Big) - \cos(Vt)\Big) + \zeta\sin\Big(\frac{s}{\lambda} + Vt\Big) \tag{25}$$

where

$$\sigma = \frac{\gamma'' L}{\zeta E J \pi n}\,. \tag{26}$$

Let us check and discuss the result. The governing equation for $s_0$ in terms of $k$ is obtained by substituting the expression for $\widetilde{H}$ given by the third equation into the first one in (20) and then by integrating over $s$. Using (21) we deduce

$$\begin{aligned}\big(m+\rho J\,Q(s_0(t))\big)\,\ddot{s}_0(t) &= \frac{EJ}{2}\left(k(s_0(t))^2-k(s_0(t)+L)^2\right)-\gamma'' L\\ &\quad -\rho J\,R(\dot{s}_0(t),s_0(t))+EJ\int_0^L \alpha(s,t)\,k_s(s_0(t)+s)\,ds \quad (27)\end{aligned}$$

where

$$\begin{aligned}R(\dot{s}_0(t),s_0(t)) &= \frac{\dot{s}_0(t)^2}{2}\left(k(s_0(t)+L)^2-k(s_0(t))^2\right)\\ Q(s_0(t)) &= \int_0^L k(s_0(t)+s)^2 ds\,.\end{aligned}$$

Equation (27) is similar to (12) with an additional term related to the longitudinal friction. The reason for this similarity relies on the analogy between the two system of equations (10) and (20), and from the fact that, if the boundary conditions (21) for the snake-like locomotion case are satisfied, then the relations between dynamical parameters at the two ends, which for the channel case are given by the boundary conditions (11), are also satisfied.

Taking now $s_0(t)=Vt$ and $k$ as stated, thanks to the $L$-periodicity of $k$, both terms $R$ and $EJ/2\left(k(s_0(t))^2-k(s_0(t)+L)^2\right)$ vanish. The same is true for the left hand side of the equation since $\ddot{s}_0=0$. The previous formula reduces to

$$EJ\int_0^L \alpha(s,t)\,k_s(s_0(t)+s)\,ds = EJ\frac{\sigma 2\pi n\zeta}{L}\int_0^L \cos\left(\frac{s}{\lambda}+Vt\right)^2 ds = \gamma'' L$$

and one can easily check that the choice (26) for $\sigma$ solves the equation. Notice that only the $s$-dependent term multiplied by $\sigma$ in the expression for $\alpha$ enters in this last relation.

Just like in the channel case, all the unknowns of the problem can be readily deduced from the knowledge of $s_0(t)$. From the third equation in (20) we can recover the expression for the shear force

$$\widetilde{H}(s,t)=\rho JV^2\frac{2\pi n}{L}\,\zeta\cos\left(\frac{s}{\lambda}+Vt\right)-\frac{2\gamma''}{\zeta}\sin\left(\frac{s}{\lambda}+Vt\right)\,,$$

while one can check that

$$\begin{aligned}\widetilde{N}(s,t) &= \frac{\gamma'' L}{4\pi n}\left(\sin 2\left(\frac{s}{\lambda}+Vt\right)-\sin 2Vt\right)\\ &\quad + \rho JV^2\frac{\zeta^2}{4}\left(\cos 2Vt-\cos 2\left(\frac{s}{\lambda}+Vt\right)\right)\end{aligned}$$

now solves the first equation in (20) and the first two boundary conditions in (21). From the second equation in (20) we can recover

$$\begin{aligned}\tilde{f} &= \gamma''\frac{L\zeta}{4\pi n}\sin\left(\frac{s}{\lambda}+Vt\right)\left(\sin 2\left(\frac{s}{\lambda}+Vt\right)-\sin 2Vt\right)-\gamma''\frac{4\pi n}{L\zeta}\cos\left(\frac{s}{\lambda}+Vt\right)\\ &+ \rho JV^2\frac{\zeta^3}{4}\sin\left(\frac{s}{\lambda}+Vt\right)\left(\cos 2Vt-\cos 2\left(\frac{s}{\lambda}+Vt\right)\right)\\ &- \rho JV^2\left(\frac{2\pi n}{L}\right)^2\zeta\sin\left(\frac{s}{\lambda}+Vt\right)-\rho AV^2\zeta\sin\left(\frac{s}{\lambda}+Vt\right)\end{aligned}$$

Finally (23) is satisfied in view of the definitions of $\alpha$ and $k$.

We remark that the expression (25) we found for $\alpha$ reflects the two effects the spontaneous curvature has in snake-like locomotion. The term multiplied by $\zeta$ in the right hand side of (25) determines the path. In fact, while this term does not enter in the equation for $s_0$, it allows to fulfil the relation $k(L,t) = \alpha(L,t) = \sin Vt$. By drawing an analogy with Section 3, this term creates at every instant a "virtual channel" in which the robot slides. In fact it has the same expression as the prescribed curvature $k$, therefore it can be seen as the spontaneous curvature required to fit the shape of the path at every instant. Since during the motion the robot must overcome the opposing frictional force, we see that another term in the expression for $\alpha$ is needed to promote forward motion. The term multiplied by $\sigma$ gives a nonzero active force in equation (27), supplying the driving force needed to slide forward in the virtual channel, therefore enabling locomotion.

Another interesting feature of (25) is that none of the reactive (external and internal) forces depend on the bending stiffness $EJ$. This allows us to discuss the rigid limit $EJ \to \infty$ (this corresponds to the problem of prescribed curvature and zero elastic flexibility, instead of prescribed spontaneous curvature with finite elastic flexibility). The observable motion and forces do not vary, while on the other hand $\alpha(s,t) \to k(s,t)$. This tells us that the inverse kinematics problem for a rigid robot with prescribed curvature can be solved in the following way: In order to move along a path producing the history of curvatures $k(s,t)$, the robot needs to replicate the exact same history with its spontaneous curvature, which in the rigid limit coincides with the observable one.

The solution obtained using (25) can be seen as the simplest example of a more general kinematic inversion scheme. It is clear from the above calculations that a spontaneous curvature $\alpha$ producing a motion such that (24) hold can be chosen between any of the type $\alpha(s,t) = \sigma\cos(s/\lambda + Vt) + \hat{\alpha}(s,t)$ with

$$\hat{\alpha}(L,t) = \zeta\sin(Vt) - \sigma\cos(Vt) \quad \text{and} \quad \int_0^L \hat{\alpha}(s,t)k_s(s,t)\,ds = 0\,. \tag{28}$$

Using the same arguments as before, the cosine term can be regarded as the "pushing" term while $\hat{\alpha}$ can be considered as the "steering" one. We show here that the extra term $\hat{\alpha}$ can be chosen to be localized in an arbitrarily small region at the leading edge, thus concentrating at the head of the robot all the effects related to the steering. Such an extra term can be taken of the form

$$\hat{\alpha}(s,t) = \begin{cases} 0 \text{ if } s \in [0, L-\delta] \\ \sum_{i=3}^{Q} p_i(t)(s-L+\delta)^i \text{ if } s \in [L-\delta, L] \end{cases} \tag{29}$$

where $\delta$ is an arbitrary small constant and $p_i(t)$ with $i = 3, \ldots, Q$ are coefficients explicitly depending on $t$ and implicitly depending also on $\delta$ and all of the other free parameters. These coefficients can be uniquely determined imposing (28) and any other $Q-5$ linearly independent relations between them (for example, in the numerical experiment we are about to propose, we imposed $\hat{\alpha}_{ss}(L,t) = 0$, which led to a smooth generated force field $\tilde{f}$ concentrated near the head). Notice that the function $\hat{\alpha}$ so defined is twice continuously differentiable. The reactive shear force and tension solving (20) can be calculated to be

$$\widetilde{H}(s,t) = \left(\rho JV^2 - EJ\right)\frac{2\pi n}{L}\,\zeta\cos\left(\frac{s}{\lambda} + Vt\right) - \frac{2\gamma''}{\zeta}\sin\left(\frac{s}{\lambda} + Vt\right) + EJ\hat{\alpha}_s(s,t)\,,$$

and

$$\begin{aligned}\widetilde{N}(s,t) &= -\sin Vt\left(EJ\zeta^2\sin Vt-\frac{\gamma^{//}L}{\pi n}\cos Vt\right)\\ &+ (\rho JV^2-EJ)\frac{\zeta^2}{4}\left(\cos 2Vt-\cos 2\left(\frac{s}{\lambda}+Vt\right)\right)\\ &+ \frac{\gamma^{//}L}{4\pi n}\left(\sin 2\left(\frac{s}{\lambda}+Vt\right)-\sin 2Vt\right)+EJ\zeta\int_0^s\sin\left(\frac{\xi}{\lambda}+Vt\right)\hat{\alpha}'(\xi,t)\,d\xi\,.\end{aligned}$$

The force exerted on the ground is, in this case,

$$\begin{aligned}\tilde{f} &= \gamma^{//}\frac{L\zeta}{4\pi n}\sin\left(\frac{s}{\lambda}+Vt\right)\left(\sin 2\left(\frac{s}{\lambda}+Vt\right)-\sin 2Vt\right)-\gamma^{//}\frac{4\pi n}{L\zeta}\cos\left(\frac{s}{\lambda}+Vt\right)\\ &+ \left(\rho JV^2-EJ\right)\frac{\zeta^3}{4}\sin\left(\frac{s}{\lambda}+Vt\right)\left(\cos 2Vt-\cos 2\left(\frac{s}{\lambda}+Vt\right)\right)\\ &- \left(\rho JV^2-EJ\right)\left(\frac{2\pi n}{L}\right)^2\zeta\sin\left(\frac{s}{\lambda}+Vt\right)-\rho AV^2\zeta\sin\left(\frac{s}{\lambda}+Vt\right) \qquad (30)\\ &- \sin Vt\left(EJ\zeta^3\sin Vt-\frac{\gamma^{//}L\zeta}{\pi n}\cos Vt\right)\sin\left(\frac{s}{\lambda}+Vt\right)\\ &+ EJ\zeta^2\int_0^s\sin\left(\frac{\xi}{\lambda}+Vt\right)\hat{\alpha}'(\xi,t)\,d\xi\sin\left(\frac{s}{\lambda}+Vt\right)+EJ\hat{\alpha}_{ss}(s,t)\,.\end{aligned}$$

We give here a graphical representation of the solution corresponding to our second example, fitting into the model the dynamical parameters relative to snake locomotion available in the literature. We choose the second example because it closely matches the experimental observations reported in [7] relative to kinematics and muscular activation during snake motion. Such measurements show that the curvature of a moving snake can be described at every time as more-or-less sinusoidal, and muscles tend to be the most active at the inflection points of the body shape. Regarding $\alpha$ as the (signed) muscular activity, we see that $\alpha(s,t)=\sigma\cos(s/\lambda+Vt)+\hat{\alpha}(s,t)$ with $\hat{\alpha}$ given by (29) fits very reasonably this picture, provided that $\delta$ is small enough.

Extrapolating the experimental values in [7] we set $L=1\text{m}$ and $\gamma^{//}=\mu^{//}mg$, where $\mu^{//}=0.2$ is the longitudinal friction coefficient, $m=1\text{kg}$ and $g$ is the gravitational acceleration constant. From the results of the same paper we choose $n=4$ and $\zeta=30\text{m}^{-1}$, the last one being the value of one local maxima (and, with opposite sign, of two local minima) of the measured snake curvature during motion. In the absence of data in the case of snakes we set $EJ=10^{-4}\text{Nm}^2$ which is the experimentally determined bending stiffness of the swimming eel present in [27]. Following [10] we neglect the inertial terms in all the expressions setting $\rho AV^2=\rho JV^2=0$. Finally, having $\delta$ no experimental analog, we assume $\delta/L=0.25$.

Four time snapshots of the resulting solution are depicted in Fig.4. Pointy segments indicate the direction and magnitude of the reactive force $\tilde{f}\mathbf{r}_s^{\perp}$ exerted by the snake on the ground. The muscular activity $\alpha$ is rendered by plotting its graph along the snake body using the midline as abscissa and the orthogonal line passing through it at each point as ordinate, then filling the region in between. The direction of the ordinate is given by $\mathbf{r}_s^{\perp}$, so that also the sign of $\alpha$ is captured.

We can see that, where the steering term of the spontaneous curvature has no effect, the force exerted on the ground always displays a local maxima (in

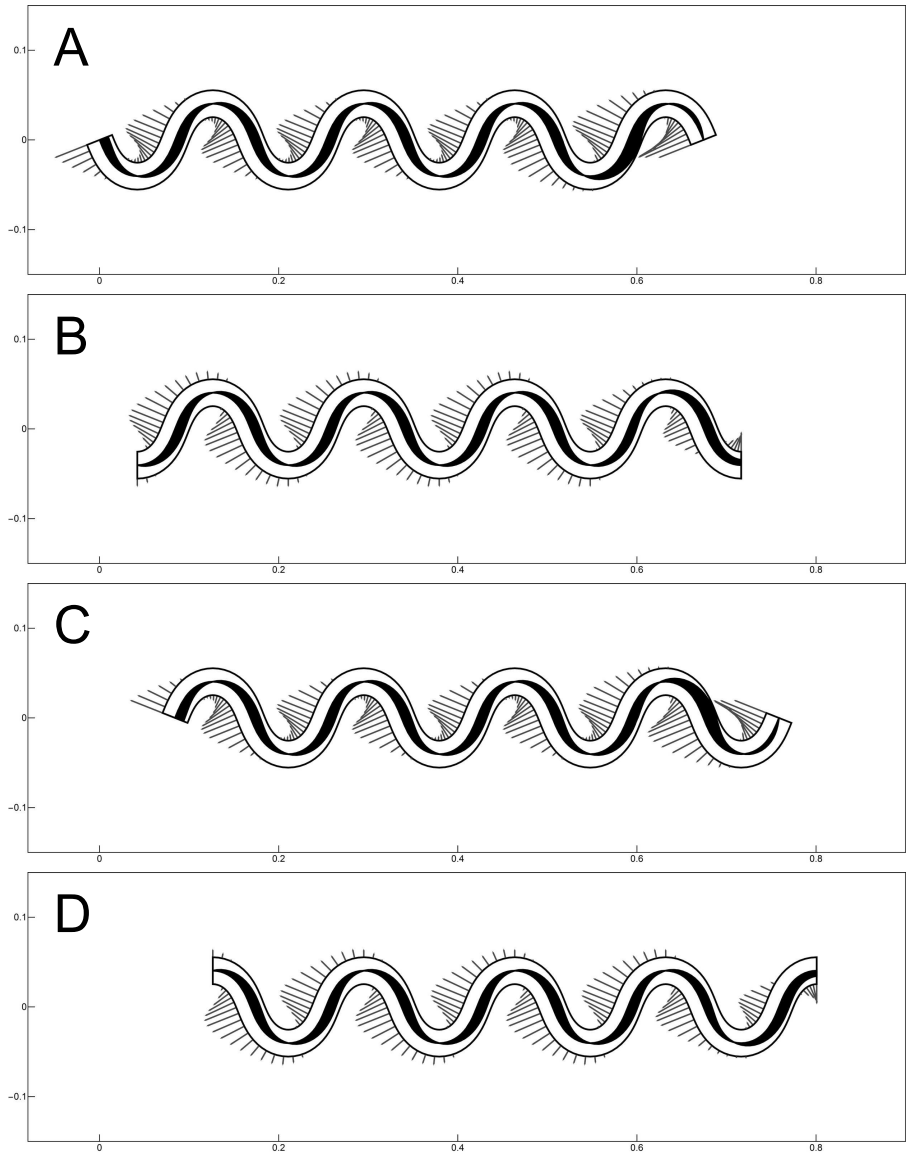


Figure 4: Snapshots for the serpentine solution at four times: A) $Vt = 0$, B) $Vt = \pi/2$, C) $Vt = \pi$ and D) $Vt = 3\pi/2$. Grey pointy segments indicate the direction and magnitude of the transversal force exerted by the snake on the ground. The muscular activity $\alpha$ is represented through the shaded areas along the snake body.

magnitude) around the inflection point of the observed curvature, in direct correlation with $\alpha$, which attains local maxima and minima at those points. This pattern is stationary with respect to an external (fixed) frame while is traveling backwards with respect to the snake body. This is in good qualitative agreement with the experimental findings in [7]. Our numerical experiments also show the break of this pattern in the proximity of the head, where the steering term of $\alpha$ is non zero. We remark that such a behaviour is due to the particular choice we made for $\hat{\alpha}$. That said, our model leads naturally to this kind of asymmetry (one cannot take $\hat{\alpha} = 0$) which, to our knowledge, has not been investigated in the experimental literature.

# 5 Discussion

We have studied the motion of a flexible elastic robot sliding in two planar constrained settings: the first consisting of a rigid, closely fitting, channel, and the second corresponding to an anisotropic frictional environment with an infinite contrast between longitudinal and transversal friction. This has led to the formulation of the equations of motion for an active Cosserat rod subjected to either the holonomic constraint (5) in the channel case, or to the nonholonomic one (16) in the second case. We were able to prove the well-posedness of both problems reducing the governing equations to an ordinary differential equation and integro-differential one, respectively.

The crucial step in proving existence and uniqueness of solutions has been the derivation of boundary conditions compatible with the external constraints, corresponding to the vanishing of the generalized edge loads. While in the channel case such edge loads are only two, in the anisotropic frictional ones they are three, resulting in an asymmetric assignment of boundary conditions. This is not surprising, giving the asymmetry between the trailing tail and the leading head but, to the best of our knowledge, this observation is new. We showed in both settings how the active spontaneous curvature of the robot can lead to propulsion. In particular we observed the active curvature having a double role in snake-like locomotion, accounting for both the pushing needed to overcome longitudinal friction, and for the steering determining the path at every instant. This double feature cannot be captured if one restricts attention to the periodic solutions considered in [12].

In our study we were able to recover and put in a quantitative framework some of the experimental observation related to snake locomotion present in the biological literature [3, 7]. The reliability of our equations, which are able to capture both internal muscular activity and force exerted by a model snake, can help further biology investigations relating internal activity and force generation in snake locomotion. The existence of explicit solutions can be also put to use in the design and motion planning of emerging bio-inspired snake-like devices [28].

Much remains to be done. First, we can think of the possibility to modify our model in order to make it closer to the physics involved in snake locomotion, considering for example an active variation of the frictional interactions between body and ground (as done in [10]). More generally, an interesting open question is why snakes move the way they do, exhibiting such recurring geometric and dynamical patterns. The direction we are currently pursuing is to extend our

analysis to the study of optimal gaits. Optimality of the gait, on the other hand, might not be the (only) determinant of real snake behaviour. Indeed, it is natural to speculate that muscular activity may be, at least to some extent, a reaction to external stimuli (the forces exerted by the ground on the snake), thereby creating a feedback mechanism between the two dynamical variables. All these questions will require further study.

**Acknowledgments** We gratefully acknowledge the support by the European Research Council through the ERC Advanced Grant 340685-MicroMotility. This work was started after an inspiring lecture given by prof. D. Bigoni at the 'Material Theories' workshop held in 2013 at the Mathematisches Forschungsinstitut Oberwolfach. ADS thanks F. Renda for useful discussions.

# References

[1] Trivedi D, Rahn C D, Kier W M, Walker I D (2008). Soft robotics: Biological inspiration, state of the art, and future research. *Applied Bionics and Biomechanics* **5.3** : 99-117. doi: 10.1080/11762320802557865

[2] Kim S, Laschi C, Trimmer B (2013). Soft robotics: a bio-inspired evolution in robotics. *Trends in Biotechnology* **31.5** : 287-294. doi: 10.1016/j.tibtech.2013.03.002

[3] Gray J (1946). The mechanism of locomotion in snakes. *Journal of Experimental Biology* **23.2** : 101-120.

[4] Gray J, Lissmann H W. (1950). The kinetics of locomotion of the grass-snake. *Journal of Experimental Biology* **26.4** : 354-367.

[5] Bekker M G (1956). Theory of Land Locomotion. *University of Michigan Press.*

[6] McNeil Akexander R (2003). Principles of Animal Locomotion. *Princeton University Press.*

[7] Moon B R, Gans C (1998). Kinematics, muscular activity and propulsion in gopher snakes. *Journal of Experimental Biology* **201.19** : 2669-2684.

[8] Baum M J, Kovalev A E, Michels J, Gorb S N (2014). Anisotropic Friction of the Ventral Scales in the Snake Lampropeltis getula californiae. *Tribology Letters* **54.2** : 139-150. doi: 10.1007/s11249-014-0319-y

[9] Berth R A, Westhoff G, Bleckmann H, Gorb S N (2009). Surface structure and frictional properties of the skin of the Amazon tree boa Corallus hortulanus (Squamata, Boidae). *Journal of Comparative Physiology A* **195.3** : 311-318. doi: 10.1007/s00359-008-0408-1

[10] Hu D L, Nirody J, Scott T, Shelley M J (2009). The mechanics of slithering locomotion. *Proceedings of the National Academy of Sciences* **106.25** : 10081-10085. doi: 10.1073/pnas.0812533106

[11] Hu D L, Shelley M J (2012). Slithering locomotion. In: Natural Locomotion in Fluids and on Surfaces, S.Childress et al. (editors), pp. 117-135, The IMA Volumes in Mathematics and its Applications. Vol **155**. *Springer-Verlag.* doi: 10.1007/978-1-4614-3997-4_8

[12] Guo Z V, Mahadevan L (2008). Limbless undulatory propulsion on land. *Proceedings of the National Academy of Sciences* **105.9** : 3179-3184. doi: 10.1073/pnas.0705442105

[13] Hirose S (1993). Biologically inspired robots: snake-like locomotors and manipulators. *Oxford University Press.*

[14] Chirikjian G S, Burdick J W (1995). The kinematics of hyper-redundant robot locomotion. *IEEE Transactions on Robotics and Automation* **11.6** : 781-793. doi: 10.1109/70.478426

[15] Boyer F, Shaukat A, Mathieu P (2012). Macrocontinuous dynamics for hyperredundant robots: Application to kinematic locomotion bioinspired by elongated body animals. *IEEE Transactions on Robotics* **28.2** : 303-317. doi: 10.1109/TRO.2011.2171616

[16] Boyer F, Porez M, Khalil W (2006). Macro-continuous computed torque algorithm for a three-dimensional eel-like robot. *IEEE Transactions on Robotics* : 563-775. doi: 10.1109/TRO.2006.875492

[17] Trivedi D, Lotfi A, Rahn C D (2008). Geometrically exact models for soft robotic manipulators. *IEEE Transactions on Robotics* **24.4** : 773-780. doi: 10.1109/TRO.2008.924923

[18] Renda F, Cianchetti M, Giorelli M, Arienti A, Laschi C (2012). A 3D steady-state model of a tendon-driven continuum soft manipulator inspired by the octopus arm. *Bioinspiration and Biomimetics* **7.2** : 025006. doi: 10.1088/1748-3182/7/2/025006

[19] Dal Maso G, DeSimone A, Morandotti M (2011): An existence and uniqueness result for the motion of self-propelled microswimmers. *SIAM J. Math. Anal.* **43**: 1345-1368 doi: 10.1137/10080083X

[20] Dal Maso G, DeSimone A, Morandotti M (2014): One-dimensional swimmers in viscous fluids: dynamics, controllability, and existence of optimal controls. *ESAIM:COCV* , in press (2014).

[21] Alouges F, DeSimone A, Giraldi L, Zoppello M (2013). Self-propulsion of slender microswimmers by curvature control: N-link swimmers. *Int.J. Nonlinear Mechanics* **56**: 142-147 doi: 10.1016/j.ijnonlinmec.2013.04.012

[22] Antman S S (2005). Nonlinear problems of elasticity. Vol **107**. *New York: Springer.*

[23] Libai A, Simmonds J G (2005). The nonlinear theory of elastic shells. *Cambridge University Press.*

[24] Bigoni D, Dal Corso F, Bosi F, Misseroni D (2014). Eshelby-like forces acting on elastic structures: theoretical and experimental proof. *Mechanics of Materials* (in press). doi: 10.1016/j.mechmat.2013.10.009

[25] Gay-Balmaz F, Vakhtang P (2012). Dynamics of elastic rods in perfect friction contact. *Physical review letters* **109.24** : 244303. doi: 10.1103/PhysRevLett.109.244303

[26] Vankerschaver J (2007). A class of nonholonomic kinematic constraints in elasticity. *Journal of Physics A: Mathematical and Theoretical* **40.14** : 3889-3913. doi: 10.1088/1751-8113/40/14/010

[27] Long, J H (1998). Muscles, elastic energy, and the dynamics of body stiffness in swimming eels. *American zoologist* **38.4** : 771-792. doi: 10.1093/icb/38.4.771

[28] Onal C D, Rus D (2013). Autonomous undulatory serpentine locomotion utilizing body dynamics of a fluidic soft robot. *Bioinspiration and Biomimetics* **8.2** : 026003. doi: 10.1088/1748-3182/8/2/026003

# Appendix. Existence and Uniqueness of Snake-Like Locomotion Solutions

For the sake of simplicity we consider the case $\rho J = 0$. The following arguments can be easily adjusted for the general case.

Let us suppose that $(s_0, k, \widetilde{N}, \widetilde{H}, \tilde{f})$ is a solution of (20) satisfying the boundary conditions (21) and the extra requirements (19) and (22) where $K(s) = k(s_0(t_0) + s)$ for $s \in [0, L]$. There is no loss of generality assuming $t_0 = 0$ and $s_0(0) = 0$. If we take $\rho J = 0$ in (27) the equation for $s_0$ in terms of $k$ is

$$m\ddot{s}_0(t) = \frac{EJ}{2}\left(k(s_0(t))^2 - k(s_0(t)+L)^2\right) - \gamma'' L + EJ\int_0^L \alpha(s,t)\, k'(s_0(t)+s)\, ds\,. \tag{31}$$

We can suppose, by restricting its domain of definition if necessary, that $s_0$ is defined on a time interval $[0, t^*)$ such that $|s_0(t)| \leq L$ for every $t \in [0, t^*)$. Within this interval the first term in the right end side of (31) reads

$$\frac{EJ}{2}\left(k(s_0(t))^2 - k(s_0(t)+L)^2\right) = \frac{EJ}{2}\left(K(s_0(t))^2 - \alpha(L,t)^2\right)\,.$$

While for the last term we have

$$\begin{aligned}
\int_0^L \alpha(s,t)\, k'(s_0(t)+s)\, ds &= \int_{s_0(t)}^{L+s_0(t)} \alpha(\xi - s_0(t), t)\, k'(\xi)\, d\xi \\
&= \int_{s_0(t)}^{L} \alpha(\xi - s_0(t), t)\, K'(\xi)\, d\xi \\
&\quad + \int_{L}^{L+s_0(t)} \alpha(\xi - s_0(t), t)\, k'(\xi)\, d\xi \\
&= \int_{s_0(t)}^{L} \alpha(\xi - s_0(t), t)\, K'(\xi)\, d\xi \\
&\quad + \int_0^t \alpha(s_0(\tau) - s_0(t) + L, t)\, \alpha(L, \tau)\, d\tau
\end{aligned}$$

where we used the change of variable $\xi = s_0(t) + s$ in the first passage and $s_0(\tau) = \xi + L$ in the second, together with the equality $k'(s_0(\tau) + L)\dot{s}_0(\tau) = \alpha(L, \tau)$ and the invertibility of $s_0$. Notice that in the last calculations we used also the fact that $\dot{s}_0 > 0$ and $s_0(t) \in [0, L]$ for every $t \in [0, t^*)$ in order to make every term meaningful, since $\alpha(s, t)$ is defined only for $s \in [0, L]$. We can see that (31) is independent from $k$ and that we can recast it into a set of integro-differential equations of the form

$$\dot{\mathbf{x}}(t) = \mathbf{G}(\mathbf{x}(t), t) + \int_0^t \mathbf{H}(\mathbf{x}(\tau) - \mathbf{x}(t), \tau, t)\, d\tau\,, \tag{32}$$

with

$$\mathbf{x}(t) = (x(t), y(t)) \ , \ \mathbf{H}(\mathbf{x}, \tau, t) = \Big( 0\,,\ \alpha(x + L, t)\, \alpha(L, \tau) \Big) \quad \text{and}$$

$$\mathbf{G}(\mathbf{x}, t) = \left( y\,,\ \frac{EJ}{2} \left( K(x)^2 - \alpha(L, t)^2 \right) - \gamma'' L + \int_x^L \alpha(\xi - x, t)\, K'(\xi)\, d\xi \right) .$$

Now, if we have a unique solution $\mathbf{x}$ of (32) with $\dot{x}(t) > 0$ and $|x(t)| \leq L$ defined for some time interval $t \in [0, t^*)$ we can set $s_0(t) := x(t)$ and

$$k(\xi) := \begin{cases} K(\xi) & \text{if } 0 \leq \xi \leq L \\ \alpha(L, x^{-1}(\xi - L)) & \text{if } L \leq \xi < L + x(t^*) \end{cases}$$

and obtain a unique solution for (31) with $|s_0(t)| \leq L$ by undoing all the previous calculations. At this point we can have two cases. Either the maximal interval of existence of $\mathbf{x}$ with $\dot{x} > 0$ is in fact $[0, t^*)$, and then the same thing holds for $s_0$, or $\mathbf{x}$ can be only defined on a closed domain $[0, t^*]$ for which $|x| \leq L$. In this last case we can still define $s_0$ and $k$ through $x$ as we did before. Then we can reapply all of the above arguments finding a solution $(s_0^1, k^1)$ of (31) with $s_0^1(t^*) = s_0(t^*)$, $\dot{s}_0^1(t^*) = \dot{s}_0(t^*)$ and $k^1(s_0^1(t^*) + s) = k(s_0(t^*) + s)$, and after that gluing the solutions together. We repeat this procedure until we reach eventually a maximal domain of existence. Once we have $s_0$ all the unknowns of (20) can be determined uniquely with the same procedure employed in Section 3. The e xistence and uniqueness of snake-like locomotion solutions then follows from the local existence and uniqueness of solutions of the integro-differential system (32), which can be proved using standard contraction mapping arguments. The result holds under the very reasonable assumption of $\alpha$ and $K$ being differentiable and uniformly bounded together with their derivatives.

We first extend $K$ and $\alpha$ outside $[0, L] \times [0, \infty)$ while keeping their regularity properties. Then we consider the Cauchy problem for (32) with initial conditions $\mathbf{x}(0) = \mathbf{x}_0$ and no extra assumption on the solutions besides differentiability. The problem can be easily proved to be equivalent to that of the existence of a fixed-point for the operator $C$ defined as

$$C\left[\mathbf{x}\right](t) = \mathbf{x}_0 + \int_0^t \left[ \mathbf{G}(\mathbf{x}(\lambda), \lambda) + \int_0^\lambda \mathbf{H}(\mathbf{x}(\tau) - \mathbf{x}(\lambda), \tau, \lambda)\, d\tau \right] d\lambda\,.$$

We restrict the operator $C$ to the space $B_{\mathbf{x}_0}^{M,T}$ of continuous vector valued functions $t \mapsto \mathbf{x}(t)$ defined on the interval $t \in [0, T]$ and such that

$$\|\mathbf{x} - \mathbf{x}_0\| = \max_{t \in [0,T]} |\mathbf{x}(t) - \mathbf{x}_0| \leq M\,.$$

There is no loss of generality assuming that the extensions we considered for $K$ and $\alpha$ lead to the existence of two constants $M_{\mathbf{G}}$ and $M_{\mathbf{H}}$ such that

$$|\mathbf{G}(\mathbf{x}(t),t)| \leq M_{\mathbf{G}} \quad \text{and} \quad |\mathbf{H}(\mathbf{x}(\tau)-\mathbf{x}(t),\tau,t)| \leq M_{\mathbf{H}} \quad \text{for every } \tau \text{ and } t$$

and for every $\mathbf{x} \in B_{\mathbf{x}_0}^{M,T}$. Also we can assume that there are other two constants $L_{\mathbf{G}}$ and $L_{\mathbf{H}}$ such that

$$|\mathbf{G}(\mathbf{x},t)-\mathbf{G}(\mathbf{y},t)| \leq L_{\mathbf{G}}|\mathbf{x}-\mathbf{y}| \quad \text{and} \quad |\mathbf{H}(\mathbf{x},\tau,t)-\mathbf{H}(\mathbf{y},\tau,t)| \leq L_{\mathbf{H}}|\mathbf{x}-\mathbf{y}|$$

for every $\tau$ and $t$ and for every $\mathbf{x},\mathbf{y} \in B_{\mathbf{x}_0}^{M,T}$. We have then

$$|\,C\,[\mathbf{x}]\,(t)-\mathbf{x}_0| \leq TM_{\mathbf{G}}+T^2M_{\mathbf{H}}$$

and also

$$\begin{aligned}
|\,C\,[\mathbf{x}]\,(t)-C\,[\mathbf{y}]\,(t)| \quad &\leq \quad \left|\int_0^t \mathbf{G}(\mathbf{x}(\lambda),\lambda)-\mathbf{G}(\mathbf{y}(\lambda),\lambda)\,d\lambda\right| \\
&+ \quad \left|\int_0^t\int_0^\lambda \mathbf{H}(\mathbf{x}(\tau)-\mathbf{x}(\lambda),\tau,\lambda)-\mathbf{H}(\mathbf{y}(\tau)-\mathbf{y}(\lambda),\tau,\lambda)\,d\tau\,d\lambda\right| \\
&\leq \quad TL_{\mathbf{G}}\,\|\mathbf{x}-\mathbf{y}\|+L_{\mathbf{H}}\int_0^t\int_0^\lambda \left|\mathbf{x}(\tau)-\mathbf{x}(\lambda)-\big(\mathbf{y}(\tau)-\mathbf{y}(\lambda)\big)\right|\,d\tau\,d\lambda \\
&\leq \quad (TL_{\mathbf{G}}+2T^2L_{\mathbf{H}})\,\|\mathbf{x}-\mathbf{y}\|\ .
\end{aligned}$$

For small enough $T$ the operator $C$ is a contraction from $B_{\mathbf{x}_0}^{M,T}$ into itself, therefore it has only one fixed point. This proves the local existence and uniqueness theorem for the extended version of (32). If we take $\mathbf{x}_0=(0,y_0)$ with $y_0>0$ then, restricting the domain of existence to an interval $[0,T^*)$ if necessary, we have by continuity $|x(t)| \leq L$ and $\dot{x}(t)=y(t)>0$ for every $t \in [0,T^*)$ obtaining therefore the unique solution to the original (non-extended) problem.